RELATIVISTIC-DFT STUDY OF THE ELECTRONIC STRUCTURE, BONDING AND ENERGETIC OF THE $[ReF_8]^-$ AND $[UF_8]^{2-}$ IONS

*WALTER A. RABANAL-LEÓN, RAMIRO ARRATIA-PÉREZ**

Facultad de Ciencias Exactas, ReMoPh Group, Universidad Andrés Bello, Av. República 275, Santiago, Chile.
(Received: July 18, 2013 - Accepted: November 19, 2013)

ABSTRACT

In this study we evaluated the importance of the relativistic effects (scalar and spin-orbit) on the description of the electronic structure, bonding and the energetic of the $[ReF_8]^-$ and $[UF_8]^{2-}$ ions. We described the bonding interaction between ligands and metal center using the energy decomposition analysis (EDA) proposed by Morokuma and Ziegler, in which it can be appreciated a strong ionic behavior for both ions since the electrostatic interaction energy ($\Delta E_{Elestat}$) is greater than the orbitalic interaction energy (ΔE_{Orb}). Furthermore, a qualitative analysis using the mapping of the electrostatic potential over the total electronic density evidence an increase of the ionic character, as well as, the polarization of the electronic density as U > Re**.** **T**he electron localization function (ELF) corroborates the bonding analysis because of the lack of di-synaptic basins on the metal-ligand bonding region.

Keywords: Hight, coordination, complexes, relativistic, effects.

INTRODUCTION

Earlier theoretical studies of the molecular structures of inorganic compounds have been carried out since 1957 using the Valence Shell Electron Pair Repulsion (VSEPR) model described by Gillepie and Nyholm[1]. This model is still used to predict qualitatively molecular geometries of main group compounds if the coordination number of six is not exceeded.[2,3]. But, what happen when coordination number is larger than six? From a theoretical point of view and on the framework of the VSEPR model, the vast majority of these cases could not have a correct prediction of the geometrical parameters for inorganic systems since the VSEPR model is rather limited due to the existence of several geometries, which are energetically close and can be interconverted by small angular changes.[3]. Despite of this, some hepta- and octa- coordinated compounds were synthetized since 1940, we can cite some examples of these high coordination compounds, such as, the homoleptic hepta-coordinated systems of Zr, Tb and U reported by W. H. Zachariasen (1949-1954)[4-6], the lanthanide hepta-fluoride systems synthetized by R. Hoppe et.al. (1961)[7,8] and also some inorganic compounds with coordination number of eight obtained by K. Seppelt and co-workers.[9-12].

Notwithstanding the large number of heavy-metal inorganic compounds with high coordination number that have been synthetized and well characterized, the theoretical research related on the description of the electronic structure, the bonding and the reactivity of this systems, especially with heavy transition-metals and rare-earths has not been completely explored.[1-6] Under all considerations made before, we performed a systematic study of the octa-coordinated compounds, $[ReF_8]^-$ and $[UF_8]^{2-}$ obtained and characterized as regular square antiprismatic structures by single crystal data by K. Seppelt et al.[7-9], in order to elucidate their electronic structure, the energetic and the nature of bonding between the fluoride ligands and the heavy transition metal or actinide center by taking into account the relevant importance of the relativistic effects (scalar and spin-orbit coupling). In this work we expect to contribute towards the understanding of the chemistry of heavy transition metal and actinide complexes.

COMPUTATIONAL DETAILS

All calculations for $[ReF_8]^-$ and $[UF_8]^{2-}$ systems were performed using the Amsterdam Density functional package (ADF)[9-11] at the non-relativistic and relativistic level of theory where the scalar and the spin-orbit coupling effects were considered by means of a two-component Hamiltonian with the zeroth order regular approximation (ZORA).[12-15]

All molecular structures were fully optimized including spin-orbit interaction via analytical energy gradient method implemented by Versluis and Ziegler[16-18] using the generalized gradient approximation (GGA) with the exchange-correlation functional proposed by Perdew-Burke-Ernzerhof (PBE)[7,19-22]. Furthermore Triple-ζ Slater basis set with two polarization functions (STO-TZ2P)[23] were used for all atoms considering a D_{4d} (D_{4d}^*) symmetry point group. In both cases a frequency analysis was carried out where we obtained only positive frequencies confirming local minima. In order to balance the effect of the high charge on the anionic systems, the Conductor like Screening Model (COSMO)[24] of solvation was employed, taking acetonitrile as solvent.

Fragment analysis in the context of the energy partitioning proposed by Morokuma-Ziegler[25,26] was performed in order to characterize the nature of the interactions involving the metal center (Re or U) and the fluoride ligands on the antiprismatic octa-coordinated complexes. Additionally to this, the electron localization function (ELF), introduced by Becke and Edgecombe[27], was also used in order to analyze the bonding interaction between the ligands and the heavy metal center, due to the ELF calculation that is a good descriptor of chemical bonding based on the topological analysis of local quantum mechanical functions related to the Pauli.[28] Finally, Voronoi[29], natural bonding orbitals (NBO)[30], quantum theory of atoms in molecules (QTAIM)[31,32] approaches were used to determine net charges to describe the possibility of charge transfer phenomena on the complexes.

RESULTS

I. Geometrical Parameters

In Table 1 are presented the calculated and experimental structural data for $[ReF_8]^-$ and $[UF_8]^{2-}$ ions, where all geometrical parameters are considered according to the Scheme depicted in Figure 1.

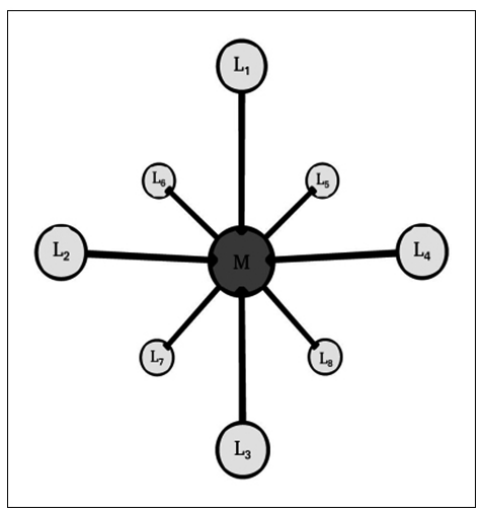

Figure 1. Selected orientation for $[ReF_8]^-$ and $[UF_8]^{2-}$ molecular structures.

e-mail. rarratia@unab.cl

For both complexes, their geometrical parameters described by scalar and spin-orbit effects are quite similar. Concerning to the calculated bond lengths and angles including relativistic effects, these are in good agreement with the experimental X-ray single crystal data with an error less than 1%. On both systems the deviation obtained for the distance and angles are slightly larger than the experimental data reported by K. Seppelt[7], which can be attributed to the direct and indirect scalar relativistic effects over s, p and d, f orbitals respectively, which modify strongly the radial part of the orbital functions specially on the valence region.

Table 1: Bond Lengths (Å) and angles (deg) for $[ReF_8]^-$ and $[UF_8]^{2-}$ complexes.

$[ReF_8]^-$				
	NR[a]	**SR[b]**	**SO[c]**	**Ref[d]**
d (M-L)	1.945	1.921	1.918	1.863 - 1.896
$<(L_2\text{-M-}L_3)$	73.07(0)	72.93(4)	72.93(5)	71.9(2)
$<(L_3\text{-M-}L_8)$	77.87(8)	78.10(5)	78.10(3)	77.6(3)
$<(L_5\text{-M-}L_7)$	114.68(3)	114.39(8)	114.40	117.7(6)
$<(L_8\text{-M-}L_9)$	142.41(0)	142.47(3)	142.47(2)	142.3(5)
$[UF_8]^{2-}$				
	NR[a]	**SR[b]**	**SO[c]**	**Ref[d]**
d (M-L)	2.184	2.156	2.152	2.070 - 2.151
$<(L_2\text{-M-}L_3)$	71.56(6)	72.21(3)	72.20(6)	72.9(2) - 73.1(2)
$<(L_3\text{-M-}L_8)$	111.56(5)	112.89(5)	112.88	112.7(2)
$<(L_5\text{-M-}L_7)$	80.37(0)	79.30(2)	79.31(4)	---
$<(L_8\text{-M-}L_9)$	143.10(4)	142.80(5)	142.80(8)	---

NR[a]: Non-Relativistic.
SR[b]: Scalar-Relativistic.
SO[c]: Spin-Orbit Relativistic.
Ref[d]: Data obtained by single crystal structure of Reference[7].

II. Electronic Structure and Molecular Orbital Analysis.

In Table 2 we show the molecular orbitals (MOs) composition and their relative energies, especially for the frontier orbitals of the $[ReF_8]^-$ and $[UF_8]^{2-}$ ions, which are also schematized in Figure 2. Moreover, the MOs energy diagrams for both ions are presented in Figure 3.

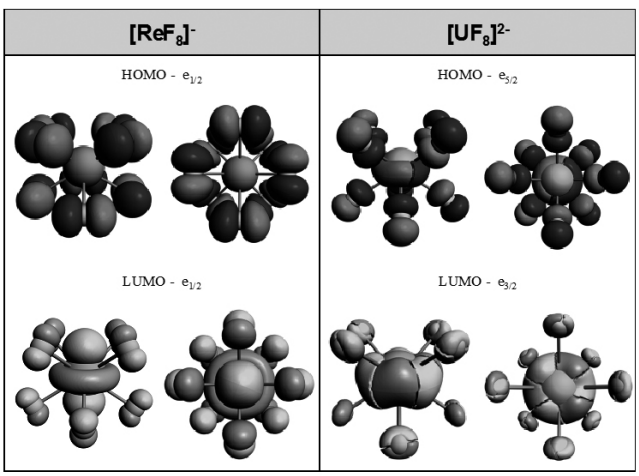

Figure 2. Frontier MOs for the $[ReF_8]^-$ and $[UF_8]^{2-}$ complexes plotted at an isovalue of 0.03 a.u.

Table 2: Molecular orbital composition and relative energies for $[ReF_8]^-$ and $[UF_8]^{2-}$ complexes obtained at Non-Relativistic (NR), Scalar-Relativistic (SR) and Spin-Orbit (SO) level.

$[ReF_8]^-$					
	E (eV)			**AOs Contributions (%)**	
	NR[a]	**SR[b]**	**SO[c]**	**NR[a]**	**SR[b]**
LUMO+3	0.2493	0.1736	-2.9390	---	---
LUMO+2	-3.2565	-2.8405	-3.5760	57.96 d_{yz} (Re) 24.99 p_x (F)	58.86 d_{yz} (Re) 23.12 p_x (F)
LUMO+1	-4.3614	-3.9563	-4.3430	58.44 d_{x2-y2} (Re) 17.37 p_z (F) 16.37 p_y (F)	60.80 d_{x2-y2} (Re) 16.34 p_z (F) 15.53p_y (F)
LUMO	-6.7501	-6.3854	-6.4020	59.65 d_{z2} (Re) 30.02 p_z (F)	62.43 d_{z2} (Re) 26.62 p_z (F)
HOMO	-8.2527	-8.2644	-8.2641	100.00 p_x (F)	100.00 p_x (F)
HOMO-1	-8.7179	-8.7271	-8.7159	52.65 p_x (F) 47.08 p_z (F)	52.55 p_x (F) 47.22 p_z (F)
HOMO-2	-8.7597	-8.7725	-8.7385	100.00 p_x (F)	100.00 p_x (F)
HOMO-3	-9.0016	-9.0111	-8.7723	53.39 p_z (F) 47.50 p_x (F)	53.17 p_z (F) 47.73 p_x (F)

$[UF_8]^{2-}$					
	E (eV)			**AOs Contributions (%)**	
	NR[a]	**SR[b]**	**SO[c]**	**NR[a]**	**SR[b]**
LUMO+3	-5.3681	-4.3548	-4.3214	68.61 f_z^3 (U) 14.60 p_z (F) 12.99 p_x (F)	76.74 f_{xyz} + f_z (U) 12.38 p_x + p_y (F)
LUMO+2	-5.4535	-4.6332	-4.8644	76.48 f_{xyz} + f_z (U) 16.74 p_x + p_y (U)	80.10 f_z^3 (U) 11.56 p_z (F)

LUMO+1	-5.6864	-4.7818	-5.0324	77.02 $f^2_{z\,x}$ + $f^2_{z\,y}$ (U) 19.92 p_x + p_y (F)	82.59 $f^2_{z\,x}$ + $f^2_{z\,y}$ (U) 10.29 p_x + p_y (F)
LUMO	-5.9135	-4.7954	-5.1059	81.49 f_x + f_y (U)	82.96 f_x + f_y (U)
HOMO	-7.1826	-7.6873	-7.6648	51.18 p_z (F) 42.57 p_x + p_y (F)	100.00 p_x (F)
HOMO-1	-7.7214	-7.9651	-7.6898	100.00 p_x (F)	100.00 p_x (F)
HOMO-2	-7.8344	-7.9869	-7.9560	73.70 p_x (F) 16.65 f^3_z (U) 10.91 p_z (U)	45.17 p_z (F) 36.52 p_x + p_y (F)
HOMO-3	-7.9889	-7.9876	-7.9799	100.00 p_x (F)	50.67 p_y + p_x (F) 49.31 p_z (F)

NR[a]: Non-Relativistic.
SR[b]: Scalar-Relativistic.
SO[c]: Spin-Orbit Relativistic.

As is expected for these systems, the highest occupied molecular orbital (HOMO) is largely localized over the fluoride ligands in both cases, this consist on the contribution of the p-orbitals from fluorine atom. The lowest unoccupied molecular orbital (LUMO) is mostly localized on each metal, but with different composition for each ion. In the case of the $[ReF_8]^-$ complex, the LUMO has a large contribution of the Re (d_{z^2}) orbital (62.43%) and a lesser contribution from the F(p_z) orbitals (26.62%). On the other hand, the LUMO in $[UF_8]^{2-}$ complex has a participation of the 5f-orbitals (82.96%) from uranium atom and a small contribution from the F(p_z) orbitals (less than ≈10% in total).

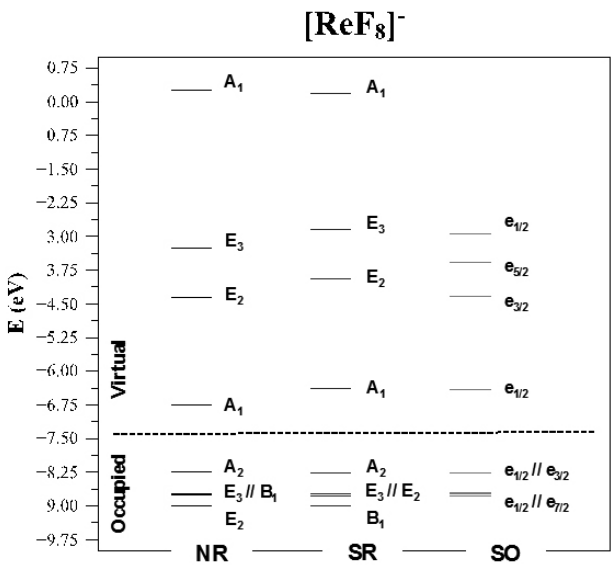

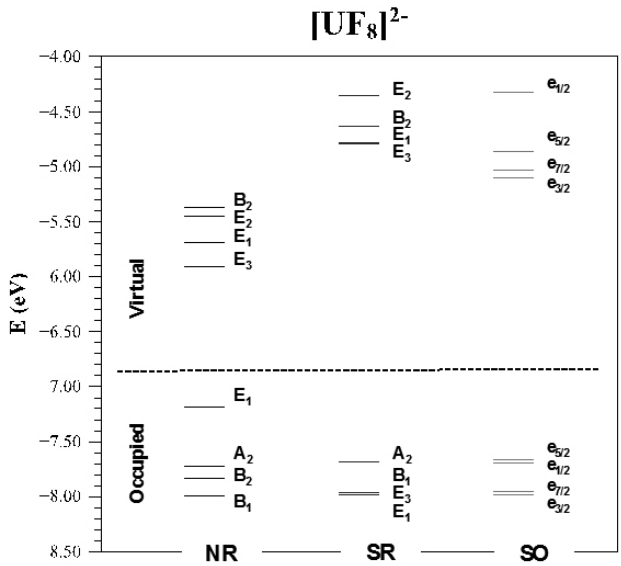

Figure 3. MOs energy diagram for $[ReF_8]^-$ and $[UF_8]^{2-}$ complexes at Non-Relativistic (NR), Scalar-Relativistic (SR) and Spin-Orbit (SO) level.

From Figure 3, it can be appreciated that the relative energy of the virtual orbitals (from LUMO to LUMO+3) in the case of scalar-relativistic calculations are destabilized as a product of the indirect relativistic effects over d and f orbitals in comparison to non-relativistic calculations, but these orbitals are re-stabilized by the spin-orbit coupling effect. Now analyzing the occupied MOs (from HOMO to HOMO-3), it can be seen the opposite behavior, the orbitals which have large contributions from the ligand (p orbital contribution) are stabilized as a product of the direct relativistic orbital contraction and this stabilization increased when the spin-orbit coupling effect is considered. For $[UF_8]^{2-}$, the stabilization or destabilization of MOs due to relativistic effects are more important than $[ReF_8]^-$ because uranium is a heavier element.

III. Bonding Nature.

In order to elucidate quantitatively the energetic of the bonding interactions, we employed the Morokuma–Ziegler energy decomposition scheme[25,26], in which the overall bond energy (ΔE) is divided in its two principal components, called "Preparation Energy" (ΔE_{prep}) and "Interaction Energy" (ΔE_{int}). In this scheme ΔE_{prep} correspond to the amount of energy required to deform the separated fragments from their equilibrium structure to the geometry that they acquire in the overall molecule, and to excite them to their valence electronic configuration. Additionally, ΔE_{int} is the energy product the steric, electrostatic and orbitalic interaction between the prepared fragments and it is composed by three physical terms described before which are: the electrostatic interaction ($\Delta V_{elestat}$), the Pauli repulsion (ΔE_{Pauli}) and the orbital interaction (ΔE_{Orb}) as indicated in equation 1.

$$\Delta E = \Delta E_{prep} + \Delta E_{int} = \Delta V_{elestat} + \Delta E_{Pauli} + \Delta E_{Orb} \quad (1)$$

In Table 3, we summarize the energy contribution involved in the $[ReF_8]^-$ and $[UF_8]^{2-}$ ions at the non-relativistic and scalar relativistic level, where the fragment-1 was considered for the metal center (Re or U) and the fragment-2 for fluoride ligands. In both cases the complexes exhibit a significant electrostatic interaction between metal center and the ligands, 65.45% for $[ReF_8]^-$ and 74.91% for $[UF_8]^{2-}$, which evidence a stronger ionic character of the Uranium complex.

Table 3: Morokuma-Ziegler energy decomposition analysis for $[ReF_8]^-$ and $[UF_8]^{2-}$ complexes obtained at Non-Relativistic (NR) and Scalar-Relativistic (SR) level in Kcal/mol.

	$[ReF_8]^-$		$[UF_8]^{2-}$	
	NR[a]	**SR[b]**	**NR[a]**	**SR[b]**
ΔE_{Pauli}	508.29	451.10	537.80	463.81
$\Delta V_{Elestat}$	-6867.93	-6858.41	-5852.92	-5837.35
ΔE_{Orb}	-3744.03	-3621.67	-2413.97	-1955.77
BE	-10103.67	-10028.97	-7729.10	-7329.30

NR[a]: Non-Relativistic.
SR[b]: Scalar-Relativistic.

The higher ionic character of the $[UF_8]^{2-}$ complex than $[ReF_8]^-$, could be due to the difference between their electronic configurations and also by the variation of the ionic radii of each metal ion. On the $[UF_8]^{2-}$ complex, the U(VI) ion, the electronic configuration looks like a noble gas $[Xe]4f^{14}5d^{10}6s^26p^65f^0 = [Rn]5f^0$, in contrast to the $[ReF_8]^-$ system in which the electronic configuration of Re(VII) ion is $[Xe]4f^{14}$ like a fully occupied trivalent lutetium ion. Here we can appreciate a different behavior of the uranium atom (5f-element) when is interacting with ligands, generally the 5f-elements tend to form molecular complexes with covalent character due to the fact that the 5f valence shell is more delocalized than the others, making these 5f-electrons available to interact with the electronic structure of the ligands. This is in contrast with 4-f elements, which have the tendency to form ionic compounds. But from the results reported in Table 3, it can be seen that $[UF_8]^{2-}$ system exhibit predominantly ionic interactions. A simple explanation for these facts could be made from the point of view of the filled of 5f-shell since we can observe that 5f-orbitals in the $[UF_8]^{2-}$ ion are empty, while 4f-orbitals are fully occupied, this idea suggest that uranium atom behaves more like an fully occupied 4f element rather than a 5f-element.

From other point of view, we can attribute the higher ionic character of the $[UF_8]^{2-}$ over $[ReF_8]^-$ as a product of the heavy atom effect phenomena which polarizes the uranium ion more than the rhenium ion giving a stronger ionic character. This effect of polarization and also the ionic character can be related with the increase of the ionic radius of the metal which is also in concordance with values of ionic radius for octa-coordinated rhenium and uranium complexes given by R. D. Shannon, which are ~0.53Å for Re (VII) and ~0.86Å for U (VI).[33]

The ELF function is defined in equation 2, as follows:

$$ELF = \left[1 + \left(\frac{C(r)}{C_h(r)}\right)^2\right]^{-1} \qquad (2)$$

Where *C(r)* has the physical meaning of the excess local kinetic energy density due to Pauli Repulsion and $C_h(r)$ is the Thomas-Fermi kinetic energy density. The ELF is a measure of the probability of finding an electron in the vicinity of a reference electron (located at a given point and with the same spin). Physically, this measure determines the spatial localization of the reference electron and provides a method for mapping the electron pair probability in multi-electronic systems.[34] In Figure 4, we plot the three-dimensional ELF function for the $[ReF_8]^-$ ion a different isovalues, in an interval from 0.2 to 0.8. Below we can observe a strong electronic localization over each nucleus of the molecular systems. The same results were found for the $[UF_8]^{2-}$ ion.

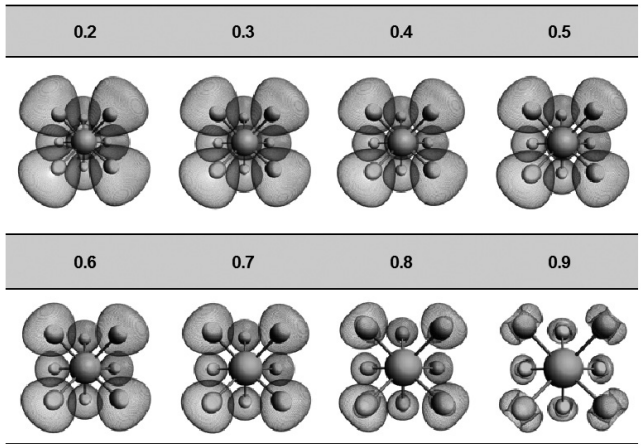

Figure 4. 3-Dimensional ELF function for the $[ReF_8]^-$ ion at [0.2 - 0.9] isovalues interval.

Finally this difference on the ionic behavior is qualitatively shown on the electrostatic potential density plot (with the same isovalue of density surface) depicted in Figure 5, where is observed a much larger polarization of charges in the $[UF_8]^{2-}$ rather than in the $[ReF_8]^-$ complex which is evidenced with an increment of the positive density on $[UF_8]^{2-}$ respect to the $[ReF_8]^-$ system.

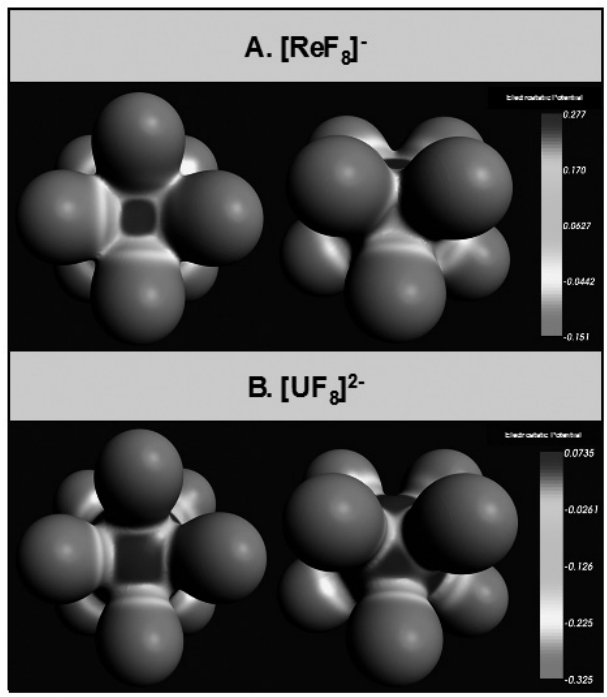

Figure 5. Electrostatic potential density plot for A) $[ReF_8]^-$ and B) $[UF_8]^{2-}$

IV. Net Charge and Charge Transfer Analysis

The calculation of charge transfer phenomena were described using different population analysis schemes like: atoms in molecules (QTAIM), the natural bonding orbital (NBO) method and Voronoi deformation density (VDD) charges, in which we evaluated the net charge of the rhenium and uranium atoms in the $[ReF_8]^-$ and $[UF_8]^{2-}$ complexes.

From the results presented in Table 4, can be appreciated for both systems that the total charge calculated with QTAIM and NBO approach on rhenium and uranium atoms, are severely underestimated with respect to the formal charge expected for these atoms considering the characteristics of the systems

with strong ionic behavior and large bond lengths. Voronoi charge population analysis is in better agreement with formal charge of the metal center. However, in the vast majority of cases the population charges analysis present a tendency with respect to the charge transfer phenomena which is described from the fluoride ligands to the metal atom. Also it is possible to appreciate that net charges obtained from non-relativistic, scalar-relativistic and spin-orbit relativistic calculations have not significantly variation among them.

Table 4: Net charge for Re and U atoms obtained at Non-Relativistic (NR), Scalar-Relativistic (SR) and Spin-Orbit (SO) level. Charge transfer (CT) was calculated at Scalar-Relativistic (SR) level.

	$[ReF_8]^-$			$[UF_8]^{2-}$		
	Voronoi	**QTAIM**	**NBO**	**Voronoi**	**QTAIM**	**NBO**
NR	3.959	3.153	2.222	4.126	2.494	1.866
SR	4.028	3.494	2.404	4.489	3.160	2.699
SO	4.029	3.495	---[b]	4.506	3.178	---[b]
CT[a]	2.972	3.506	4.596	1.494	2.822	3.301

[a] Charge transfer was calculated as follows : CT = 7 – q(Re) or CT = 6 – q(U),where q(Re) and q(U) are the net charge over Re and U atoms (the numbers 7 and 6 refers the formal charge of the Rhenium and Uranium ions, respectively) .

[b] There is not an available algorithm at the spin-orbit relativistic level.

It is well-known that in chemical systems with strong ionic character the presence of high charge transfer help to stabilize energetically the systems, this can be appreciated for the $[ReF_8]^-$ and $[UF_8]^{2-}$ complexes by taking the bonding energy (BE) as a measurement of the stability as deduced from the Morokuma-Ziegler energy decomposition analysis given in Table 3, which present huge values of BE on the framework of the scalar-relativistic calculations for both systems, giving values of -7329.30 kcal/mol and -10028.97 kcal/mol for $[ReF_8]^-$ and $[UF_8]^{2-}$, respectively. Nevertheless, we must remember that the charge population analysis methods are sensitive to the basis set choice on the vast majority of cases.[35]

CONCLUSIONS

Our results suggest a good agreement between the relativistic calculations and the available structural data with an error less than 1% for bond lengths and angles. The electronic structure show that the highest occupied molecular orbital (HOMO) has entirely contribution from p_x AO from fluoride ligands, whereas the lowest unoccupied molecular orbital (LUMO) show strong contributions from d (~59.44%) and f (81.31%) of rhenium and uranium AOs, respectively. The scalar and spin-orbit relativistic effects induce an increment of the HOMO-LUMO (H-L) gap, being the $[UF_8]^{2-}$ H-L gap (2.56 eV) higher than the $[ReF_8]^-$ H-L gap value (1.86 eV). The H-L gap value is directly related with the stability of the systems and also corroborates the results of the bonding energy from the EDA.

Furthermore, the results obtained from the EDA evidence a strong ionic interaction between fluoride ligands and the metal center (rhenium or uranium) since the electrostatic interaction energy ($\Delta E_{Elestat}$) is greater than orbitalic interaction energy (ΔE_{Orb}) for $[ReF_8]^-$ and $[UF_8]^{2-}$. Moreover, the ionic character increases according to U > Re, which is in concordance with the electrostatic potential density plot and also with the increment on the bond lengths from $[ReF_8]^-$ to the $[UF_8]^{2-}$ ion. All the facts above mentioned and in addition to the high variation of the net charge and the out of phase MOs interaction suggest a spatial charge transfer phenomena possibly mediated by a Föster mechanism.[36]

The electron localization function (ELF) confirms the result presented above by showing localized monosynaptic basins over fluoride ligands and metal centers. The absence of di-synaptic basins on the M-F bond also suggests the lack of overlap interaction.

ACKNOWLEDGEMENTS

This work is dedicated to Professor Juan Guillermo Contreras Koder.

The authors acknowledge financial support of projects UNAB-DI-404-13/I, UNAB-DI-292-13/R, Fondecyt 1110758. W.R. acknowledges financial support for Ph.D. studies from AGCI and CONICYT-PCHA/Doctorado Nacional/2013-63130118 fellowship.

REFERENCES

1. Arratia-Pérez, R.; Hernandez-Acevedo, L.; Malli, G. L. *J. Chem. Phys.* **2004**, *121*, 7743.
2. Gillespie, R. J. *Coordination Chemistry Reviews* **2008**, *252*, 1315–1327.
3. Arratia-Pérez, R.; Malli, G. L. *J. Chem. Phys.* **2006**, *124*, 074321.
4. Páez-Hernández, D.; Ramírez-Tagle, R.; Codorniu-Hernández, E.; Montero-Cabrera, L. A.; Arratia-Pérez, R. *Polyhedron* **2010**, *29*, 975–984.
5. Páez-Hernández, D.; Murillo-López, J. A.; Arratia-Pérez, R. *J. Phys. Chem. A* **2011**, *115*, 8997–9003.
6. Ferraro, F.; Barboza, C. A.; Arratia-Pérez, R. *J. Phys. Chem. A* **2012**, *116*, 4170–4175.
7. Hwang, I.-C.; Seppelt, K. *Journal of Fluorine Chemistry* **2000**, *102*, 69–72.
8. Seppelt, K. *Comments on Inorganic Chemistry* **1991**, *12*, 199–211.
9. Keplert, D. L. *Inorganic Stereochemistry*; 1st ed. Springer Berlin Heidelberg: Berlin, 1982; Vol. 6.
10. ADF2010, SCM, Theoretical Chemistry, Vrije Universiteit, Amsterdam, The Netherlands, http://www.scm.com.
11. Velde, te, G.; Bickelhaupt, F. M.; Baerends, E. J.; Fonseca Guerra, C.; van Gisbergen, S. J. A.; Snijders, J. G.; Ziegler, T. *J. Comput. Chem.* **2001**, *22*, 931–967.
12. Lenthe, E. V.; Baerends, E. J.; Snijders, J. G. *J. Chem. Phys.* **1993**, *99*, 4597.
13. Zachariasen, W. H. *Acta Cryst (1949) Q2, 60-62* **1949**, 1–3.
14. Zachariasen, W. H. *Acta Cryst (1954) Q7, 783-787 [doi:101107/S0365110X54002447]* **1954**, 1–5.
15. Zachariasen, W. H. *Acta Cryst (1954). Q7, 792-794 [doi:10.1107/S0365110X54002460]* **1954**, 1–3.
16. Versluis, L.; Ziegler, T. *J. Chem. Phys.* **1988**, *88*, 322.
17. Hoppe, R.; Liebe, W. *Zeitschrift für anorganische und allgemeine Chemie* **1961**, *313*, 221–227.
18. Hoppe, R.; Rödder, K. M. *Zeitschrift für anorganische und allgemeine Chemie* **1961**, *312*, 277–281.
19. Perdew, J.; Burke, K.; Ernzerhof, M. *Phys. Rev. Lett.* **1996**, *77*, 3865–3868.
20. Mahjoub, A. R.; Seppelt, K. *Angewandte Chemie International Edition in English* **1991**, *30*, 876–878.
21. Giese, S.; Seppelt, K. *Angewandte Chemie International Edition in English* **1994**, *33*, 461–463.
22. Adam, S.; Ellern, A.; Seppelt, K. *Chemistry-A European Journal* **1996**, *2*, 398–402.
23. Van Lenthe, E.; Baerends, E. J. *J. Comput. Chem.* **2003**, *24*, 1142–1156.
24. Pye, C. C.; Ziegler, T. *Theor Chem Acc* **1999**, *101*, 396–408.
25. Kitaura, K.; Morokuma, K. *Int. J. Quantum Chem.* **1976**, *10*, 325–340.
26. Ziegler, T.; Rauk, A. *Theoretica Chimica Acta* **1977**, *46*, 1–10.
27. Becke, A. D.; Edgecombe, K. E. *J. Chem. Phys.* **1990**, *92*, 5397–5403.
28. Savin, A.; Jepsen, O.; Flad, J.; Andersen, O. K.; Preuss, H.; Schnering, von, H. G. *Angewandte Chemie International Edition in English* **1992**, *31*, 187–188.
29. Fonseca Guerra, C.; Handgraaf, J.-W.; Baerends, E. J.; Bickelhaupt, F. M. *J. Comput. Chem.* **2004**, *25*, 189–210.
30. Reed, A. E. *J. Chem. Phys.* **1983**, *78*, 4066.
31. Rodríguez, J. I.; Bader, R. F. W.; Ayers, P. W.; Michel, C.; Götz, A. W.; Bo, C. *Chemical Physics Letters* **2009**, *472*, 149–152.
32. Rodríguez, J. I. *J. Comput. Chem.* **2013**, *34*, 681–686.
33. Shannon, R. D. *Acta Crystallographica Section A: Crystal Physics, Diffraction, Theoretical and General Crystallography* **1976**, *32*, 751–767.
34. Savin, A.; Nesper, R.; Wengert, S.; Fässler, T. F. *Angewandte Chemie International Edition in English* **1997**, *36*, 1808–1832.
35. Philips, J. J.; Hudspeth, M. A.; Browne, P. M., Jr.; Peralta, J. E. *Chemical Physics Letters* **2010**, *495*, 146–150.
36. Förster, T. *Discuss. Faraday Soc.* **1959**, *27*, 7.